



Simulating vehicle dynamics on both design plans and laser-scanned road geometry to guide highway design policy



Alexander Brown ^{a,*}, Sean Brennan ^b

^a Penn State University, 336D Reber Building, University Park, PA 16802, United States

^b Mechanical Engineering, Penn State University, 157D Hammond Building, University Park, PA 16802, United States

ARTICLE INFO

Article history:

Received 1 February 2014

Received in revised form 28 June 2014

Accepted 29 July 2014

Available online 27 August 2014

Keywords:

Model validation

Roadway construction

Mapping

Data collection

Simulation

Highway safety

Design guidance

Vehicle dynamics

ABSTRACT

Increasingly, roadway designers use simulations to analyze how roadway design choices affect vehicle dynamics and ultimately safety. When using commercial multi-body simulations for analysis of vehicle dynamics, engineers are usually able to trust that the vehicle states predicted by simulations are reasonably accurate. This is because simulation software companies spend significant research and development dollars making sure that vehicle models and numerical solvers give realistic results. However, when using vehicle dynamic simulations for the analysis of roadway designs, the road environment must be defined by the user. Researchers are often left to wonder whether the roads they simulate in software are representative of what construction crews actually built in the field. This paper compares the results of simulations using both a road's design geometry, i.e., the CAD plans, versus a three-dimensional point-cloud scan of its actual geometry. For this comparison, high-fidelity commercial vehicle simulation software (CarSim and TruckSim) was used. Research-grade sensing equipment allowed for the digitization of road geometries during highway traversals in the field to create a simulated mesh of the real highway geometry. After comparing simulation results for traversals of design geometry and measured road geometry with collected vehicle data, the road safety implications of discrepancies seen between the predicted and measured vehicle states are also discussed.

© 2014 Elsevier Ltd. All rights reserved.

1. Introduction

The study that follows is a small portion of a large three-year effort funded by the National Cooperative Highway Research Program (NCHRP 15-39) to investigate current highway design policies for sharp horizontal curves and steep downgrades. The project looked at the current American Association of State Highway and Transportation Officials (AASHTO) highway design specifications (AASHTO, 2011), and how a range of highway geometries designed to these specifications affected the chances of single-vehicle skidding and rollover-related accidents occurring for a wide range of vehicle designs, and a range of braking, lane-change, and curve following scenarios. While a large portion of this study consisted of vehicle simulations of the above scenarios, the project also included an instrumented vehicle study to determine the suitability of five current roadways designed to AASHTO standards. Because correct representation of three-dimensional road geometry is paramount to accurate simulation of vehicle dynamics, as is clear from prior work in road profile measurement (Chemstruck

* Corresponding author.

E-mail addresses: aab5009@psu.edu (A. Brown), sbrennan@psu.edu (S. Brennan).

et al., 2009; Dembski et al., 2006; Detweiler and Ferris, 2010; Kern and Ferris, 2007; Stine et al., 2010), examination of these sites included both a data collection and a simulation component.

This paper summarizes the methodology used for obtaining real-world roadway geometry measurements for comparison to designed road geometry. While any driving situation could be simulated, the primary focus of this paper is to assess vehicle dynamics on real highway curve traversals during normal (non-emergency) operation. First, a set of field experiments was conducted in which the dynamic states of a full-sized SUV were collected using a defense-grade Inertial Navigation System (INS) while the test vehicle followed free-flowing highway traffic around a horizontal curve on a steep downgrade. This was repeated for 7 consecutive traversals of the road segment of interest, for 5 different measurement sites across 2 states. While collecting vehicle measurements, a high-fidelity Light Distance And Ranging (LIDAR) sensor mounted on the vehicle recorded a three-dimensional point cloud representing the geometry of the road. This point cloud was then processed to generate a roadway mesh geometry. Then, simulations of a vehicle traversing the road defined by the LIDAR-measured geometry were performed in CarSim. The simulated vehicle was given the same longitudinal target speed profile as the test vehicle measured in the field. Finally, using the same longitudinal speed profile, a second simulation was performed on a road represented by the curve's *design* geometry, e.g. the Computer-Aided Design (CAD) geometry provided by the state DOT representing the design as it was built according to AASHTO policy. This procedure is outlined in Fig. 1.

The paper provides discussions of how the simulated geometries were prepared for use in CarSim, how the test vehicle and procedure were prepared, summarizes results for multiple roadways in the northeastern United States including discrepancies in geometries, and gives detailed results for selected sites to illustrate the simulation and data processing procedure. The analysis of the data from the three sources of data (measured, simulated on real road, simulated on road design geometry) shows good agreement between the simulation outputs generated by both CAD geometry and the collected data. Finally, the paper concludes with recommendations to others performing this type of research in future road safety studies.

2. Data collection methodology

Roadway geometry, cross-slope, and vehicle dynamic data were collected at five locations from in-vehicle sensors while the test vehicle followed free-flow vehicles through the sites. At each site, data were collected while following behind five separate passenger vehicles and two tractor semi-trailers. The goal of this vehicle shadowing process was to measure and thereby replicate a statistical picture of the normal traffic encountered at each roadway. This enabled simulations to use the measured speed profile of a vehicle traversing the road geometry in question, rather than a guessed or idealized speed profile, in evaluating the road's safety characteristics.

The test vehicle, a 2010 Dodge Durango, was chosen because of its capacity to hold the data collection equipment, and because the vehicle's inertial and kinematic parameters align well with those defined as a standard full-size SUV within CarSim. The vehicle was instrumented with a defense-grade Global Positioning System (GPS) (2 m 2-sigma position) coupled to a ring-laser-gyro Inertial Measurement Unit (IMU) that provided accurate low-drift absolute measures of position and orientation. The GPS/IMU data were collected at 100 Hz. Additionally, a roof-mounted Light Detection And Ranging (LIDAR) was mounted on a gantry behind and above the vehicle with the sensor facing vertically and perpendicular to the road. This road-scanning system gave 180 degree cross-section measurements of the road surface at 0.5 degree intervals, out to a distance of 260 ft from the sensor, for a total of 361 points per sweep. Each sweep was repeated at 37.5 Hz while capturing the infrared reflectivity of the surface impinged by the laser and returning a representative intensity value.

In addition to the LIDAR sensor, a color camera was mounted to the dashboard of the vehicle and manually aligned so that the vanishing point of straight-line driving corresponded roughly to the center of the image. Finally, a steering angle sensor

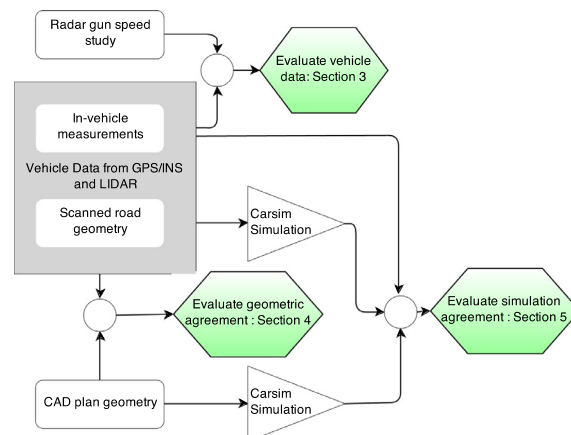


Fig. 1. Outline of methodology for comparison of vehicle simulations between design plans and laser-scanned geometry.

captured the driver's steering inputs directly. All sensor data were collected using Player/Stage software, and each measurement was time-stamped by the computer's local clock (Gerkey et al., 2003). A diagram of the data collection system is shown in Fig. 2, and an example screen shot from the forward-facing camera on the dashboard is shown in Fig. 3, showing a snapshot of the heads-up display of data being collected from the sensing equipment.

During each data collection run, the vehicle's pilot drove a fixed distance behind vehicles in the traffic stream chosen randomly but selected such that the followed vehicles were "free-flowing," which implies that the followed vehicle was sufficiently isolated and not influenced by other cars or trucks around it in its speed behavior. The instrumented vehicle maintained a constant following distance of approximately 300 ft behind the lead vehicle as shown in Fig. 3. Selected vehicles were followed beginning at the top/bottom of the grade and followed down/up the entire grade and throughout the curve. The data collection system provided very accurate readings on a range of data, including:

Vehicle data:	Roadway data:
<ul style="list-style-type: none"> • Velocities on each of the three axes • Acceleration/deceleration on each of the three axes • Steering angle • Roll, pitch, and yaw angles and rates about each axis 	<ul style="list-style-type: none"> • Vertical alignment • Horizontal alignment • Normal cross-slope • Transition from normal cross-slope to full superelevation • Full superelevation in curve
<ul style="list-style-type: none"> • Position of the vehicle in latitude, longitude, and elevation 	

3. Evaluation of vehicle speed and acceleration data

Simulation predictions of vehicle states and friction utilization from CAD or LIDAR geometry were a large part of the highway design investigation that instigated the present study, so it was important to determine whether one geometry produced more accurate simulation results. The trust in these comparisons assumes the use of a statistically probable vehicle traversal. To check the validity of the speed measurements, Fig. 4 shows six of the speed traces (one outlier removed) from the instrumented vehicle traversals at the WV2 site in West Virginia. Additionally, plots of the position-correlated mean speeds measured using road-side laser guns which were used to measure hundreds of vehicle speeds throughout the curve. This particular site had full coverage of the curve from the roadside laser gun locations. All speed traces measured by the instrumented vehicle fell within two standard deviations of the mean speed measured by road-side laser guns (see Fig. 5).

Fig. 4 illustrates some interesting phenomena of a typical passenger vehicle entering a curve (Bonneseon, 1999). For example, the instrumented vehicle study showed that most vehicles that were followed maintained relatively constant speeds through the curve, punctuated by areas of short speed changes. This behavior was readily observed in most of the traversals. For some vehicles, however, there are very large speed changes within the curve. For example, Fig. 4 shows a situation where one followed vehicle changed speed from approximately 80 mph before the curve, to 50 mph within the curve, and then back to 80 mph after the curve.

Fig. 4 shows the corresponding acceleration/deceleration of the subject vehicles while traversing the data collection site, as measured from the instrumented vehicle. Shown in this figure are the individual data traces for each vehicle traversal, the mean acceleration at each point in the curve, and the upper and lower bounds created from two standard deviations from the mean at each location. Prior work by Bonneseon (1999) suggested that vehicles slow down slightly on the entrance to a curve, with very minor deceleration rates of -3 ft/s^2 . This deceleration on the entrance to curve was not conclusively or consistently seen in the speed data collected from the instrumented vehicle at any of the five sites; indeed, many of the "followed



Fig. 2. Instrumented vehicle data collection system.



Fig. 3. Screenshot from Instrumented vehicle during data collection.

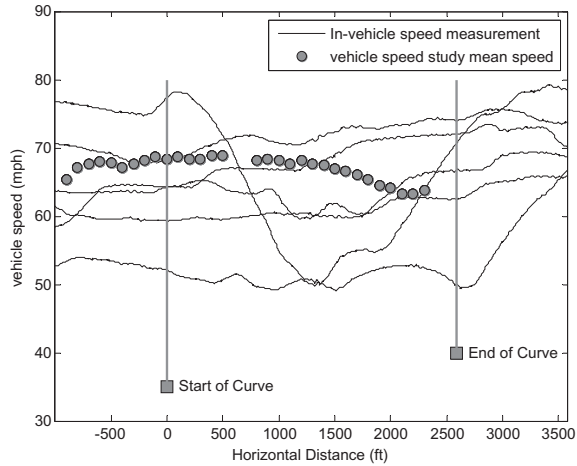


Fig. 4. Comparison of speed profiles from instrumented vehicle and mean speeds from laser guns at Cheat Lake, WV (site WV2).

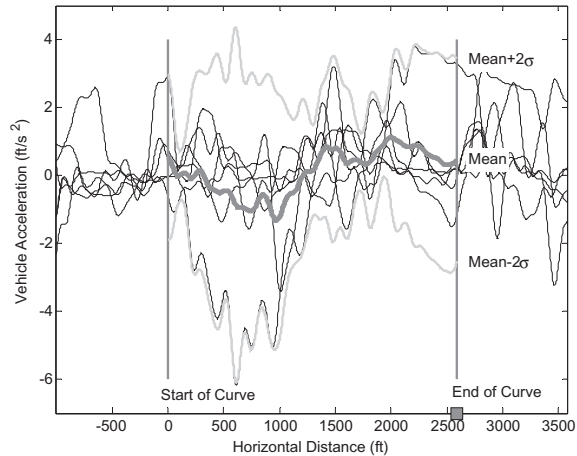


Fig. 5. Longitudinal acceleration profiles from instrumented vehicle in Cheat Lake, West Virginia (site WV2).

vehicles” actually accelerated slightly rather than decelerated upon entrance to the curve. However, the upper and lower bounds on the accelerations throughout the curve are approximately bounded by 3 ft/s² deviations from zero acceleration (e.g., constant speed), consistent with the variations seen in the Bonneson study.

Several general findings regarding the speed data collected from the instrumented vehicle are as follows:

- Overall, the mean speed profiles measured by the instrumented vehicle agreed with the speed data collected from the laser guns. For the entire WV2 site, laser gun measured speed had a standard deviation of 5.9 mph, which indicates that the speed traces from the in-vehicle measurements were statistically consistent.

- The variability in the vehicle acceleration within a curve was approximately between 3 and -3 ft/s^2 . While this variation occurred throughout the curve, the acceleration magnitude is consistent with the curve entry deceleration reported by [Bonneson \(1999\)](#).

4. Comparison of measured roadway geometry with cad plans

For each data collection site, the researchers worked with the state agencies and highway construction authorities to obtain copies of each site's design geometry, provided as a table of measured road grade, cross-slope, and horizontal geometry values. For this study, these tables represent an "ideal" representation of the road. Simple hand measurements of cross-slope and grade as obtained from a slope meter were available, but it was quickly seen that these measurements only reflect isolated "snapshots" of the road geometric variability as constructed versus as idealized. To make sure every ripple and imperfection in the road surface could be accounted for in subsequent simulations, a more detailed map of road geometry was necessary.

To paint an accurate picture of the three-dimensional geometry of the road surface as it was actually constructed, roadway geometry data were obtained from the LIDAR range measurements. Standard coordinate transformations were used to convert from LIDAR coordinates to vehicle coordinates, and finally to globally-referenced coordinates (see [Vemulapalli and Brennan \(2009\)](#) for details). The resulting point-cloud data were filtered to develop a smoothed road profile that provided grade, with interpolation methods employed as in [Varunjikar \(2011\)](#). As a result of these 3-D data processing steps, horizontal alignment and cross-slope information was provided for each site. An example illustration of the resulting road profile after processing is shown in [Fig. 6](#).

One of the first confirmations conducted on the measured data was to verify that the measured grades matched the grades as reported on profile sheets for the sites. As an example, the measured grades were inferred from the elevation versus horizontal alignment measurements as shown in [Fig. 7](#) for the Cheat Lake, WV site labeled "WV2." In [Fig. 7](#) (and all subsequent figures), the zero point along the horizontal alignment depicts the beginning of the curve (i.e., PC). Positive values for the horizontal distance represent the relative position along the length of the curve, and negative values represent the relative position along the approach tangent to the curve. In [Fig. 7](#) the inferred grade from field measurements is $-5.62 \pm 0.22\%$, which is consistent with the grade obtained from the profile sheets for this same site, -5.7% . A similar level of consistency between measured grades and grades obtained from profile sheets occurred across all five sites in the instrumented vehicle study (see [Table 1](#)).

The second level of consistency checks focused on horizontal alignment. The measured horizontal alignment of the Cheat Lake, West Virginia site is shown [Fig. 8](#). The figure illustrates a curve to the left. Through visual inspection, comparisons were made of the collected horizontal geometry versus the CAD drawings of the road plans. Additionally, the collected horizontal vehicle trajectory was compared to Google Earth satellite images to further confirm geometric consistency visually. These comparisons indicated a high level of agreement between the instrumented vehicle data and the actual roadway plans.

Visual inspection confirmed that the in-vehicle geometric measurements agreed well with horizontal and vertical alignment information obtained from roadway plans and profiles, so the horizontal and vertical alignment data from CAD geometries were imported into CarSim. The vehicle motion through the curve was simulated to obtain predicted vehicle dynamic behavior. These pitch and roll predictions from CAD profiles were then compared to instrumented vehicle measurements. An example of this comparison is shown in [Fig. 9](#) for the Cheat Lake, West Virginia site "WV2." One can observe that the simulation outputs closely agree with the measured data, including many of the transient effects such as oscillations in the entry and exit of the curve. Note that the disagreement up to -500 m is due to the acceleration of the instrumented vehicle to match the velocity of selected vehicles within free-flow traffic prior to the curve entry.

The confirmation that the simulation outputs closely agreed with the data from the instrumented vehicle was important in several respects. First, it confirmed the fidelity and/or accuracy of the CarSim model for use in subsequent phases of the highway design study. Second, it provided confidence that that horizontal and vertical alignment and cross-slope/superel-

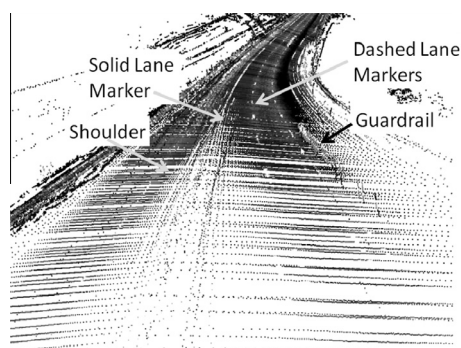


Fig. 6. 3-D point cloud obtained by instrumented vehicle data, Friendsville, MD (site MD1).

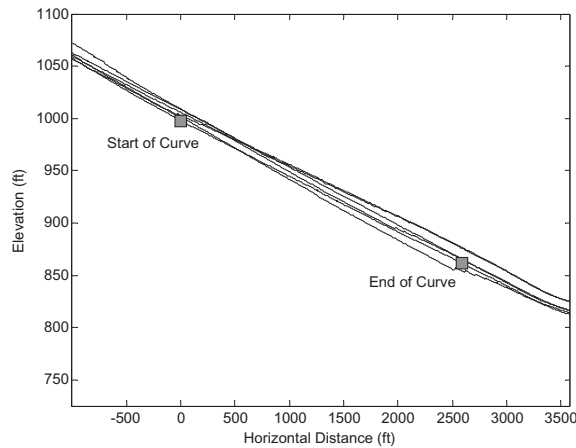


Fig. 7. Measured elevations and horizontal distance for all traversals at Cheat Lake, West Virginia (site WV2).

Table 1
Comparison of grades from instrumented vehicle data and profile sheets.

Site name	Site info		Percent grade	
	Route	Nearest city	Measured	CAD plans
MD1 ¹	I-68 Westbound	Friendsville , MD	-4.07 ± 0.27	-4.1
MD2	I-68 Westbound	Hancock, MD	6.17 ± 0.33	6.0
MD3	I-68 Westbound	Hancock, MD	-5.61 ± 0.25	-5.7
PA1 ¹	I-79 Northbound	Washington, PA	-5.19 ± 0.16	-5.0
WV2	I-68 Westbound	Cheat Lake, WV	-5.62 ± 0.22	-5.7

¹ Slope for approach is different than the curve. The values shown are for approach.

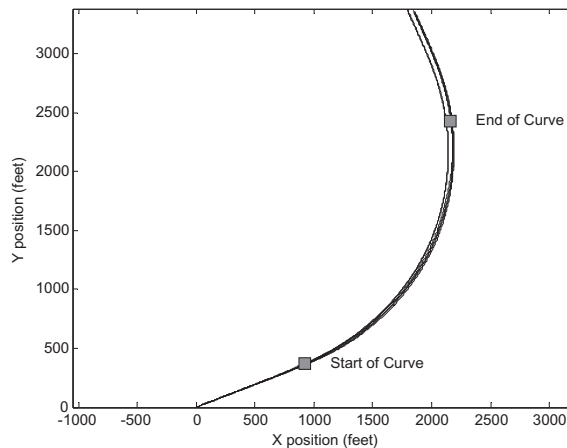


Fig. 8. Horizontal alignment from instrumented vehicle for all traversals at Cheat Lake, West Virginia (site WV2).

evaluation data obtained from combinations of plans and profiles, roadway inventory files, and field measurements could be used to accurately model the geometrics of the 20 data collection sites within CarSim, without the need to use the instrumented vehicle to collect this information for every site.

While these are important results, the question of whether the LIDAR-generated geometrics are equally suitable for use in vehicle simulations remains. In the event that a road as it is actually constructed does *not* match its CAD plans, a researcher wishing to investigate the road in question for safety concerns must have a way to accurately model the road for simulation purposes. This is addressed in the following section.

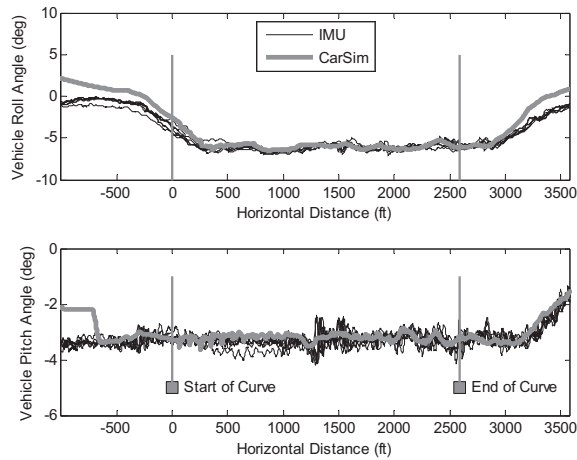


Fig. 9. Comparison of CarSim simulation results and instrumented vehicle inertial measurement unit (IMU) measurements for all traversals at Cheat Lake, West Virginia (site WV2).

5. Comparison of CarSim simulation results for cad geometry vs. measured lidar geometry

The preceding section showed the agreement between measured road grade during data collection runs, and showed that the collected vehicle orientation matched closely with a simulation of the same using the road's CAD plans as geometric inputs to CarSim. However, to determine the efficacy of using a LIDAR-generated geometric mesh for vehicle dynamic simulations, an evaluation is necessary comparing CAD plans to field LIDAR measurements as respective road-geometry inputs to simulations on vehicle traversals.

To this end, simulations comparing vehicle states resulting from each geometry generation method were performed for each of the six data collection sites to confirm agreement. Using states with high signal-to-noise ratios, such as pitch and roll, offered an illustrative comparison. An example comparison between the pitch and roll values using the two different geometry sources for the Cheat Lake, West Virginia site is shown in Fig. 10. Because the pitch and roll values measured from the instrumented vehicle roughly correspond with the grade and superelevation of the road, with vehicle sprung mass motion added, this provides yet another comparison of the two methods of generating roadway geometry for simulation.

Fig. 10 is time-aligned rather than distance-aligned since vehicle dynamic data are strongly time-dependent. It shows a general agreement between the two methods of geometry generation, with Root-Mean-Squared Difference (RMSD) values of less than 1/10 of a degree for both roll and pitch. The LIDAR-generated geometry is considerably rougher than the CAD plans, which can be accounted for by considering roadway construction methods, highway wear, and LIDAR/INS sensor noise. However, Fig. 10 indicates that the road was designed to specification, with the possible exception of errors in construction of the transition in road grade at the start of the curve at this site, and an apparent deviation in vehicle roll angle at the end of the curve.

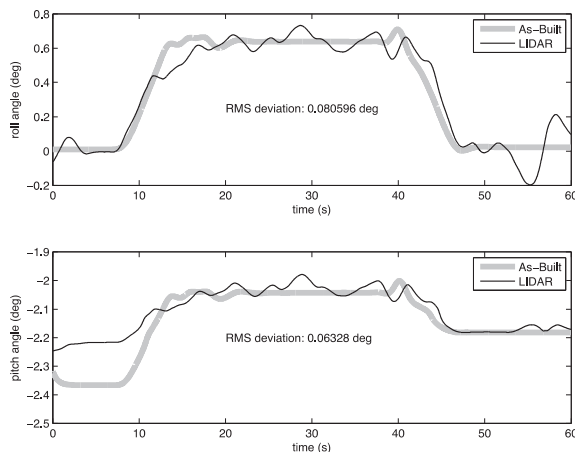


Fig. 10. Comparison of CarSim simulation results using LIDAR-generated and CAD-generated geometry for vehicle orientation at Cheat Lake, West Virginia (site WV2).

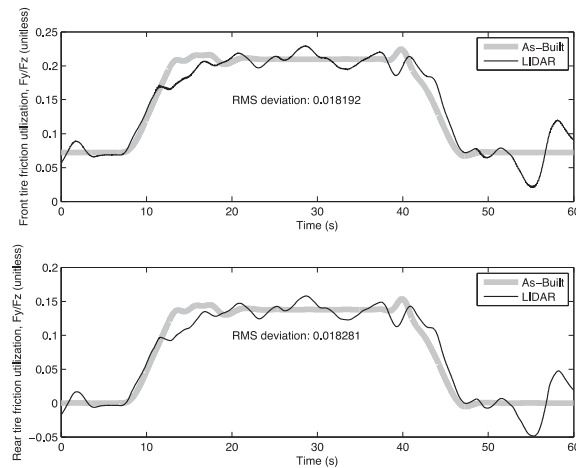


Fig. 11. Comparison of CarSim simulation results using LIDAR-generated and CAD-generated geometry for vehicle friction usage at Cheat Lake, West Virginia (site WV2).

To track down the sources of each of these areas of disagreement, consider that the Cheat Lake, West Virginia site “WV2” is a curve at the bottom of a long downgrade. The curve itself has a less severe downgrade than the straight section preceding it. While this is reflected in both simulations in Fig. 10, the grade transition is different in construction than specified in the design plans. This rather complex geometry could have easily been modified during roadway construction, and its relatively minor error magnitude – coupled with the fact that errors are evident only around transitions of geometry – supports the hypothesis of construction-related changes. Similarly, the curve’s end, in its transition from a fully superelevated curve to normal drainage superelevation, shows some disagreement. Inspection of the video from this traversal indicates that the test vehicle was forced to change lanes at the end of the curve to maintain following distance with the followed, free-flow vehicle, which means that a lane change was “built-in” to this measured geometry, and then fed into the simulation. This lane change maneuver introduces sufficient body roll as to explain the discrepancy. The fact that this relatively minor maneuver still showed up in the road geometry emphasizes the sensitivity of the measurement equipment used for mapping the roadway.

Many of the sites considered had similar exceptions to a general rule of good geometric agreement, which led to an investigation, in a vehicle-dynamic sense, of the relative importance of the observed discrepancies between measured road geometry and CAD plans.

For each site, to determine whether LIDAR-generated geometries and CAD plans gave substantially different results in a way that could affect simulations relating to road safety, vehicle friction utilization was compared between each of the geometry methods to provide a numerical measure of how the vehicle “sees” the geometric differences. Because tire friction usage is a direct measure of the proximity of a vehicle to a sliding condition as in Pacejka (2005), these states are the most illustrative when considering the relative impact of using measured vs. CAD geometry. A comparison between each geometry method is shown in Fig. 11.

The observed friction factors are low (close to AASHTO design values) for each of the two simulations in Fig. 11, which highlights just how small the differences are in friction factor between LIDAR-measured and CAD generated road geometry, and downplays the observed geometric differences. RMS differences between the simulations’ predicted tire force usage are roughly 0.018 for each tire, or just over 10% of the maximum friction used in this maneuver. The “built-in” lane change in the LIDAR-generated geometry is also visible in Fig. 11 at the end of the curve, but it is also obviously a very minor part of the overall picture, given that the friction factor deviation caused by the lane change is only about 1/3 the magnitude of the total friction factor generated at the apex of the turn.

The deviations observed in geometry and in friction utilization bring up an interesting point about the data collection method itself: because the centerline of the “measured road geometry” was defined as the vehicle’s position during the mapping procedure, care must be taken during mapping to avoid lane changes and other maneuvers that could alter the resulting geometric profile. Alternatively, the LIDAR data could be post-processed to extract lane lines from intensity data after conversion to global coordinates, which would give an absolute measure of the lane center independent of vehicle motion. Nevertheless, the results above indicate that for the Cheat Lake, West Virginia site “WV2,” and similarly for many of the other sites considered in the NCHRP 15-39 study, either CAD geometry or LIDAR-measured geometry could be used to generate legitimate road profiles for vehicle dynamic simulations.

6. Conclusions

Consistent with the main goals of the instrumented vehicle study, there are several observations that can be inferred through the analysis of results presented above. First, the speed profiles of the instrumented vehicle study were found to

be in agreement with the speed data collected from the laser guns. In addition, the magnitude of the decelerations observed from the instrumented vehicle speed data is consistent with the findings of NCHRP Report 439 by [Bonneson \(1999\)](#).

Second, the roll and pitch outputs from the vehicle dynamics simulations agreed closely with the instrumented vehicle data. This agreement gave the research team confidence in the fidelity of the simulation results, offering confirmation of the simulation software's fidelity when simulations were run on CAD road geometry.

Lastly, the horizontal and vertical alignment and cross-slope/superelevation data obtained from combinations of plans and profiles, roadway inventory files, and field measurements agreed with the corresponding data measured from the instrumented vehicle, and simulations conducted on LIDAR-generated geometry agreed with simulations conducted on CAD geometry. Because plans and profiles, roadway inventory files, and rough field measurements were available for all 20 data collection sites, and the instrumented vehicle results and LIDAR geometry were available only at 5 sites, horizontal and vertical alignment and cross-slope/superelevation data obtained from combinations of plans and profiles were used for all site-specific simulations in the full NCHRP highway design study. This was only possible because the LIDAR-generated geometry results agreed so closely with CAD geometry results for all sites measured.

Acknowledgements

The authors gratefully acknowledge the support of the National Academy of Science Transportation Research Board, Project 15–39, in supporting portions of this study.

References

- American Association of State Highway and Transportation Officials, 2011. *A Policy on Geometric Design of Highways and Streets*, Washington, DC
- [Bonneson, J.A., 1999. Side friction and speed as controls for horizontal curve design. *J. Transp. Eng.* 125 \(6\), 473–480.](#)
- [Chemistruck, H.M., Detweiler, Z.R., Ferris, J.B., Reid, A., Gorsich, D., 2009. Review of current developments in terrain characterization and modeling, modeling and simulation for military operations IV. In: Dawn A. Trevisani \(Ed.\), *Proceedings of SPIE*, Vol. 7348, 73480N.](#)
- [Dembski, N., Rizzoni, G., Soliman, A., Malmmedahl, G., Disaro, L., 2006. The development of a terrain severity measurement system. *Proc. ASME IMECE*.](#)
- [Detweiler, Z.R., Ferris, J.B., 2010. Interpolation methods for high-fidelity three-dimensional terrain surfaces. *J. Terramech.* 47 \(4\), 209–217.](#)
- [Gerkey, B.P., Vaughan, R.T., Howard, A., 2003. The player stage project: tools for multi-robot and distributed sensor systems. *Proceedings of International Conference on Advanced Robotics*, Coimbra, Portugal, pp. 317–323.](#)
- [Kern, J., Ferris, J., 2007. Development of a 3-D vehicle-terrain measurement system part i: equipment setup, *Proceedings of the Joint North America Asia-Pacific ISTVS Conference and Annual Meeting of Japanese Society for Terramechanics*, Fairbanks.](#)
- [Pacejka, H., 2005. *Tire and Vehicle Dynamics*. Elsevier.](#)
- [Stine, J.S., Hamblin, B.C., Brennan, S.N., Donnell, E.T., 2010. Analyzing the influence of median cross-section design on highway safety using vehicle dynamics simulations. *Accid. Anal. Prev.* 42 \(6\), 1769–1777.](#)
- [Varunjikar, T., 2011. Design of horizontal curves with downgrades using low-order vehicle dynamics models, mechanical engineering, University Park, The Pennsylvania State University, Master of Science.](#)
- [Vemulapalli, P., Brennan, S.N., 2009. Design and testing of a terrain mapping system for median slope measurement. *Proceedings of the Transportation Research Board of the National Academy of Science*, Washington, DC.](#)